fractal and fractional

MDPI

Article

The Effect of Caputo Fractional Variable Difference Operator on a Discrete-Time Hopfield Neural Network with Non-Commensurate Order

Rabia Chaimaà Karoun [1,*], Adel Ouannas [2], Mohammed Al Horani [1] and Giuseppe Grassi [3]

[1] Departement of Mathematics, The University of Jordan, Amman 11942, Jordan
[2] Departement of Mathematics and Computer Science, The University of Larbi Ben M'hidi, Oum El Bouaghi 04000, Algeria
[3] Dipartimento Ingegneria Innovazione, Universita del Salento, 73100 Lecce, Italy
* Correspondence: karoun.ch13@gmail.com

Abstract: In this work, we recall some definitions on fractional calculus with discrete-time. Then, we introduce a discrete-time Hopfield neural network (D.T.H.N.N) with non-commensurate fractional variable-order (V.O) for three neurons. After that, phase-plot portraits, bifurcation and Lyapunov exponents diagrams are employed to verify that the proposed discrete time Hopfield neural network with non-commensurate fractional variable order has chaotic behavior. Furthermore, we use the 0-1 test and C_0 complexity algorithm to confirm and prove the results obtained about the presence of chaos. Finally, simulations are carried out in Matlab to illustrate the results.

Keywords: Hopfield neural network; fractional variable order; chaos; bifurcation; Lyapunov exponents; C_0 complexity; 0-1 test

Citation: Karoun, R.C.; Ouannas, A.; Horani, M.A.; Grassi, G. The Effect of Caputo Fractional Variable Difference Operator on a Discrete-Time Hopfield Neural Network with Non-Commensurate Order. *Fractal Fract.* **2022**, *6*, 575. https://doi.org/10.3390/fractalfract6100575

Academic Editors: Ivanka Stamova, Gani Stamov and Xiaodi Li

Received: 10 September 2022
Accepted: 5 October 2022
Published: 9 October 2022

1. Introduction

Recently, due to its multiple applications, particularly in the context of secure communication [1–4] and control [5,6], chaotic discrete-time systems have gained a lot of attention. Lozi map [7], 2-D Hénon system [8], Zeraoulia-Sprott map [9], Baier–Klein map [10], the generalized Hénon system [11] and the discrete Rössler system [12] are a few examples of chaotic discrete-time systems with integer order that have been presented over time. Researchers have lately become more interested in the systems with fractional order that correspond to the previous chaotic systems with integer order [13].

Fractional-order derivatives are more precise than integer-order derivatives because they are a great tool for describing the memory effect in a variety of materials and processing [14].

Discrete fractional calculus and fractional difference operators have received the attention of mathematicians [15–17]. Refs. [18,19] introduced the concept of discrete fractional calculus to chaotic maps and showed that chaos characteristics remain. For instance, in [20], the authors analysed the existence of chaos in 2D maps with fractional order, the chaotic behavior of Ikeda map with a non-integer order was studied in [21], in [22], fractional chaotic systems with discrete time and without equilibrium points were introduced, and, in [23], bifurcation and dynamics of systems with fractional and various closed curve equilibrium points were investigated, while control and dynamics of fractional quadratic map with no equilibrium points were analysed in [24].

The great interest of taking into account a Caputo fractional difference operator [25] in the modeling of dynamical systems with discrete time was demonstrated by the pertinent publications cited above.

Since fractional calculus has more advantages than an integer one, it makes sense for us to use this approach in studying neural networks' systems [26–29]. The modeling of neural networks with fractional order is used to investigate biological neurons for two

reasons. First, by increasing one degree of freedom, the fractional order increases the performance of the system. Second, the modeling of neural networks with fractional order has an infinite memory. Fractional-order neural networks hope to play an important role in the field of parameter estimation. Neural networks approximation showed higher rates of approximation at a fractional level [30].

A lot of attention has been paid to the analysis of the dynamics of neural networks with fractional order, and significant results have been achieved. For instance, in [31], LMI conditions for global stability of fractional-order neural networks were studied; in Ref. [32], the authors presented an adaptive model-free synchronization of different fractional-order neural networks with an application in cryptography, the stability, bifurcation, and chaos of Hopfield neural networks with a non-integer order were analysed. In [33–37], the stability of the Hopfield neural networks with fractional order was investigated, in [38], complexity, chaos and multi-stability of a discrete time Hopfield neural network with variable order and short memory were studied, whereas, in [39], the dynamics of the fractional order neural network were analysed. Recently, in [40], a study of discrete time Hopfield neural network with incommensurate fractional order was presented.

The major purpose of this research is to study the effect of using the non-commensurate fractional variable-order on the system studied in [40]. The fractional variable-order form is likely to exhibit even more complex dynamics.

Inspired by the research cited above, firstly, a discrete time Hopfield neural network with a non-commensurate fractional variable order is proposed. Then, the dynamics of the presented model are analysed via phase-plot portraits, bifurcation and maximum Lyapunov exponent (MLE) diagrams. After that, 0-1 test and the C_0 complexity algorithm are used to confirm the chaotic behavior of the system. Finally, the corresponding simulations are performed.

2. Preliminaries on Discrete Fractional Calculus

In this section, we present some definitions according to fractional discrete calculus to describe the discrete time Hopfield neural network (D.T.H.N.N.) with an incommensurate fractional variable-order.

Discrete Fractional Calculus

Let h be a function defined on a time scale $\mathbb{N}_\beta = \{\beta, \beta+1, \beta+2, ...\}$.

- The η-th fractional sum for the function h is defined as [16]:

$$\Delta_\beta^{-\eta} h(r) = \frac{1}{\Gamma(\eta)} \sum_{\rho=\beta}^{r-\eta} (r-\rho-1)^{(\eta-1)} h(\rho), \quad r \in \mathbb{N}_{\beta+\eta}, \eta > 0, \tag{1}$$

where

$$(r-\rho-1)^{(\eta-1)} = \frac{\Gamma(r-\rho)}{\Gamma(r-\rho-\eta+1)}, \tag{2}$$

which represents the falling factorial function.

- The η-Caputo fractional difference operator for the function h is defined as [25]:

$${}^C\Delta_\beta^\eta h(r) = \Delta_a^{-(k-\eta)} \Delta^k h(r), \tag{3}$$

where $k = [\eta] + 1$, $r \in \mathbb{N}_{\beta+k-\eta}$, and $\eta \notin \mathbb{N}$.

Using the Formulas (1) and (2), we obtain:

$$ {}^{c}\Delta_{\beta}^{\eta} h(r) = \frac{1}{\Gamma(k-\eta)} \sum_{\rho=\beta}^{r-(k-\eta)} \frac{\Gamma(r-\rho)}{\Gamma(r-\rho-k-\eta+1)} \Delta_{\rho}^{k} h(\rho), \tag{4} $$

where Δ_{ρ}^{k} is the k-th integer difference operator defined as:

$$ \Delta^{k} h(r) = \Delta(\Delta^{k-1} h(r)) = \sum_{j=0}^{k} \binom{k}{j} (-1)^{k-j} h(r+j), \qquad r \in \mathbb{N}_{\beta}. \tag{5} $$

3. The Discrete-Time Neural Network with an Incommensurate Fractional Variable Order

Sivasundaram and Kaslik [41] described the model of the Hopfield fractional neural network consisting of m neurons as follows:

$$ {}^{c}D^{\gamma_j} x_j(r) = -\alpha_j x_j(r) + \sum_{j=1}^{m} A_{j,i} h_j(x_i(r)) + E_j, \quad \forall r > 0, \ \ \forall j = 1, 2, ..., m. \tag{6} $$

Given that:

- $h_j : \mathbb{R} \to \mathbb{R}$ represents the activation function of the neurons;
- $A = (A_{ji})_{m \times m}$ denotes the weights matrix which describes the connection between i and j neurons;
- $\alpha_j > 0$ represents the self-regulating neurons' parameters;
- E_j are the external inputs; in our work, they are equal to 0.

Note that ${}^{c}D^{\gamma_j}$ is the Caputo fractional order derivative defined as:

$$ {}^{c}D^{\gamma_j} h(r) = \frac{1}{\Gamma(1-\gamma_j)} \int_{r_0}^{r} (r-\rho)^{-\gamma_j} h(\rho) d\rho, \tag{7} $$

where the fractional order $\gamma_j \in (0, 1]$.

Here, we consider a system with three neurons. To simplify calculations, herein choose $h_j(x_i) = tanh(x_i)$, $\alpha_j = 1$, and the matrix A is chosen as:

$$ A = \begin{bmatrix} -1.4 & 1.2 & -7 \\ 1.1 & 0 & 2.8 \\ P & -2 & 4 \end{bmatrix}. \tag{8} $$

As a result, we obtain the following Hopfield neural network with continuous time:

$$ \begin{cases} {}^{c}D^{\gamma_1} x_1(r) &= -x_1(r) - 1.4 tanh(x_1(r)) + 1.2 tanh(x_2(r)) - 7 tanh(x_3(r)), \\ {}^{c}D^{\gamma_2} x_2(r) &= -x_2(r) + 1.1 tanh(x_1(r)) + 2.8 tanh(x_3(r)), \\ {}^{c}D^{\gamma_3} x_3(r) &= -x_3(r) + P tanh(x_1(r)) - 2 tanh(x_2(r)) + 4 tanh(x_3(r)). \end{cases} \tag{9} $$

From system (9), we obtain a new D.T.H.N.N with incommensurate fractional variable-order by replacing the operator ${}^{c}D^{\gamma_i}$ with the Caputo-like difference operator with fractional variable-order ${}^{c}\Delta^{\gamma_i(r)}$, which can be given by:

$$\begin{cases} {}^{c}\Delta^{\gamma_1(r)}x_1(r) = -x_1(r+\gamma_1(r)-1) - 1.4tanh(x_1(r+\gamma_1(r)-1)) + 1.2tanh(x_2(r+\gamma_1(r)-1)) \\ \qquad\qquad -7tanh(x_3(r+\gamma_1(r)-1)), \\ {}^{c}\Delta^{\gamma_2(r)}x_2(r) = -x_2(r+\gamma_2(r)-1) + 1.1tanh(x_1(r+\gamma_2(r)-1)) + 2.8tanh(x_3(r+\gamma_2(r)-1)), \\ {}^{c}\Delta^{\gamma_3(r)}x_3(r) = -x_3(r+\gamma_3(r)-1) + Ptanh(x_1(r+\gamma_3(r)-1)) - 2tanh(x_2(r+\gamma_3(r)-1)) \\ \qquad\qquad +4tanh(x_3(\tau+\gamma_3(r)-1)), \end{cases} \tag{10}$$

with $r \in \mathbb{N}_{\beta+1-\gamma_j(r)}$, $\gamma_j(r)$ being the variable order and $\gamma_j(r) \in (0,1]$, $j = 1,2,3$.

3.1. Dynamical Analysis and Numerical Simulations

The goal of this section is to illustrate the dynamics of the D.T.H.N.N with incommensurate fractional variable order (10) via numerical simulation.

Now, according to the theorem cited in [42], the unique solution of the system (10) is given by:

$$\begin{cases} x_1(r) = x_1(\beta) + \frac{1}{\Gamma(\gamma_1(r))} \sum\limits_{\tau=\beta+1-\gamma_1(r)}^{r-\gamma_1(r)} (r-\tau-1)^{(\gamma_1(r)-1)}\{-x_1(\tau+\gamma_1(r)-1) \\ \quad -1.4tanh(x_1(\tau+\gamma_1(r)-1)) + 1.2tanh(x_2(\tau+\gamma_1(r)-1)) - 7tanh(x_3(\tau+\gamma_1(r)-1))\}, \\ x_2(r) = x_2(\beta) + \frac{1}{\Gamma(\gamma_2(r))} \sum\limits_{\tau=\beta+1-\gamma_2(r)}^{r-\gamma_2(r)} (r-\tau-1)^{(\gamma_2(r)-1)}\{-x_2(\tau+\gamma_2(r)-1) \\ \quad +1.1tanh(x_1(\tau+\gamma_2(r)-1)) + 2.8tanh(x_3(\tau+\gamma_2(r)-1))\}, \\ x_3(r) = x_3(\beta) + \frac{1}{\Gamma(\gamma_3(r))} \sum\limits_{\tau=\beta+1-\gamma_3(r)}^{r-\gamma_3(r)} (r-\tau-1)^{(\gamma_3(r)-1)}\{-x_3(\tau+\gamma_3(r)-1) \\ \quad +Ptanh(x_1(\tau+\gamma_3(r)-1)) - 2tanh(x_2(\tau+\gamma_3(r)-1)) + 4tanh(x_3(\tau+\gamma_3(r)-1))\}. \end{cases} \tag{11}$$

Take $\beta = 0$ and since $(r-\tau-1)^{(\gamma_j(r)-1)} = \frac{\Gamma(r-\tau)}{\Gamma(r-\tau-\gamma_j(r)+1)}$, and the numerical formula of the system (10) is designed as:

$$\begin{cases} x^1_{n+1} &= x^1_0 + \sum\limits_{j=0}^{n} \frac{\Gamma(n-j+\gamma_1(j))}{\Gamma(\gamma_1(j))\Gamma(n-j+1)}\{-x^1_j - 1.4tanh(x^1_j) + 1.2tanh(x^2_j) - 7tanh(x^3_j)\}, \\ x^2_{n+1} &= x^2_0 + \sum\limits_{j=0}^{n} \frac{\Gamma(n-j+\gamma_2(j))}{\Gamma(\gamma_2(j))\Gamma(n-j+1)}\{-x^2_j + 1.1tanh(x^1_j) + 2.8tanh(x^3_j)\}, \\ x^3_{n+1} &= x^3_0 + \sum\limits_{j=0}^{n} \frac{\Gamma(n-j+\gamma_3(j))}{\Gamma(\gamma_3(j))\Gamma(n-j+1)}\{-x^3_j + Ptanh(x^1_j) - 2tanh(x^2_j) + 4tanh(x^3_j)\}, \end{cases} \tag{12}$$

with the known initial condition $x^1_0 = x_1(0)$, $x^2_0 = x_2(0)$, $x^3_0 = x_3(0)$.

To study the effect of the fractional variable order on the D.T.H.N.N (10), we take $P = 0.57$ and the initial condition $(x^1_0, x^2_0, x^3_0) = (0, 0.01, 0)$, where the fractional variable order is chosen as: $\gamma_1(r) = tanh(r)$, $\gamma_2(r) = \frac{1}{1+e^{-r}}$ and $\gamma_3(r) = \frac{r}{1+r}$.

Firstly, we draw the discrete time evolution of the states as shown in Figure 1.

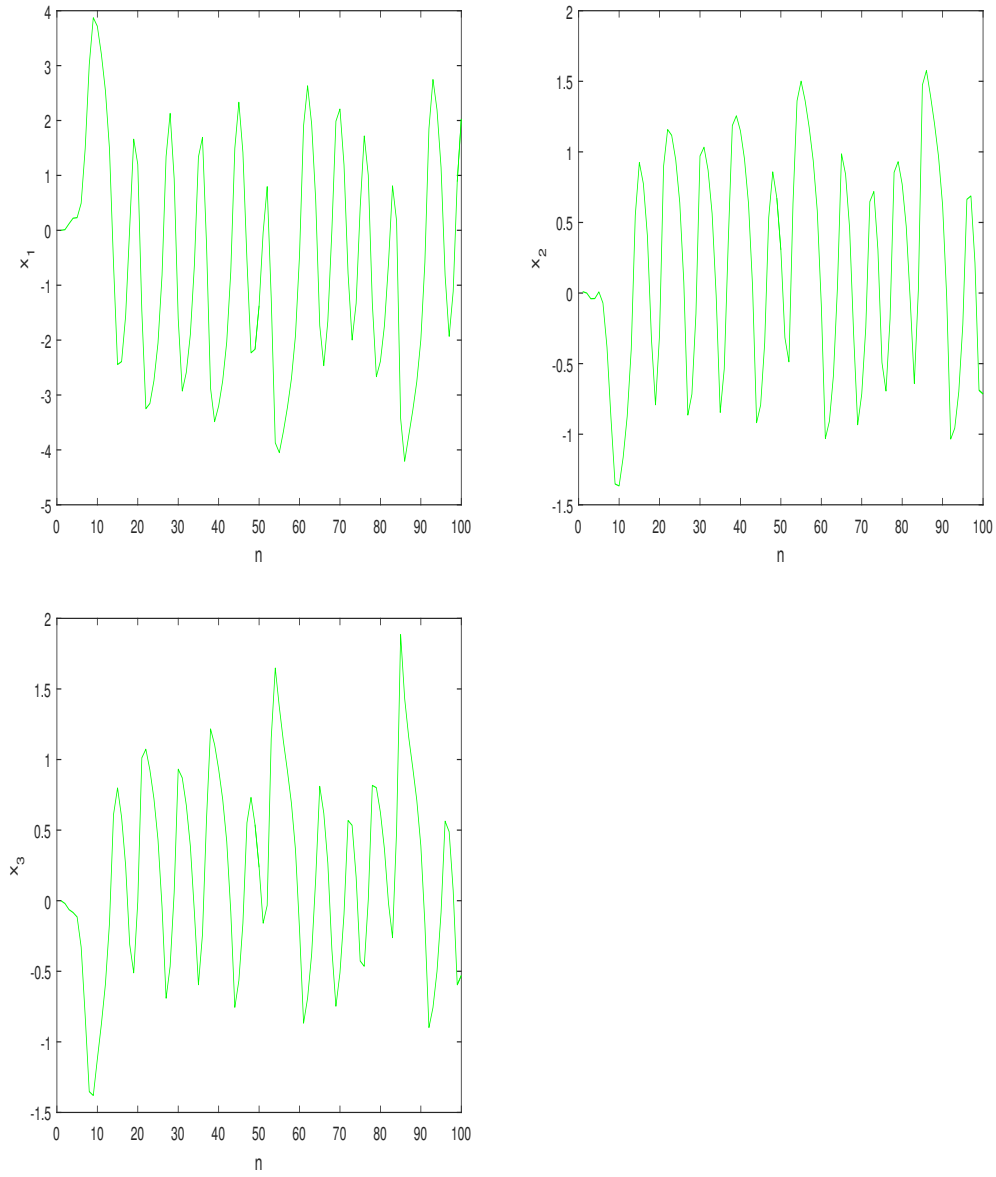

Figure 1. Time evolution of the states x_1, x_2 and x_3 of the D.T.H.N.N with incommensurate fractional V.O (10).

We observe that the states x_1, x_2 and x_3 of the system (10) exhibit chaotic behaviour, but we do not rely on it to determine the nature of the dynamic; for this reason, we need to plot the trajectories in the state space.

Figure 2 depicts the plot of phase portraits of our system (10), which displays a chaotic attractor.

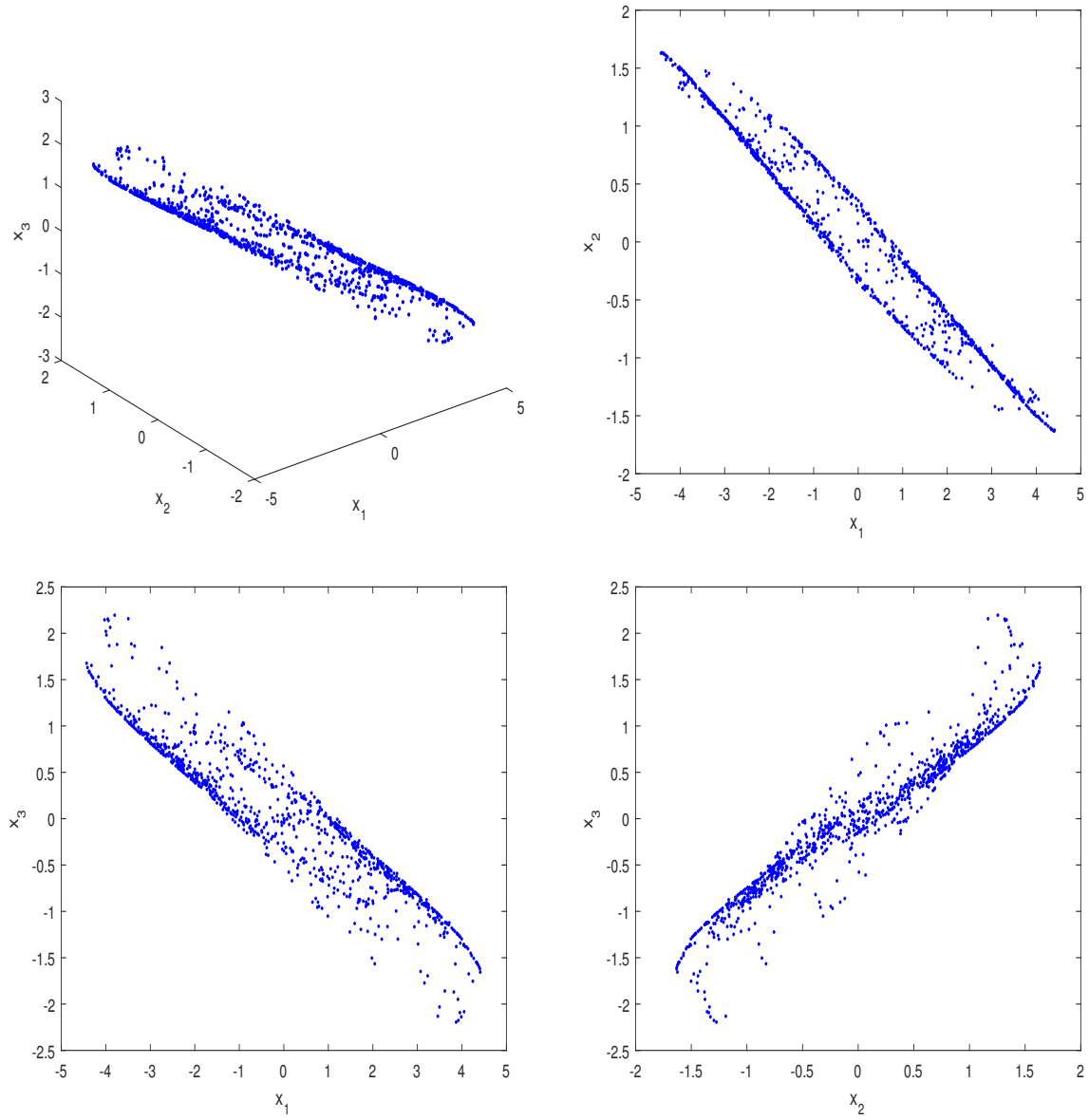

Figure 2. Phase-plot portraits of the D.T.H.N.N with incommensurate fractional variable-order (10).

3.2. Bifurcation Diagram and Maximum Lyapunov Exponents

Now, in order to explore the presence of chaos, we consider the bifurcation diagram and maximum Lyapunov exponents of the state x_1 by varying the parameter P in the interval $[0, 1.5]$ with the step $\Delta P = 0.0025$. Note that we calculate the maximum L.E using the algorithm of Jacobian matrix [43].

In our case, the matrix J_j of the system (10) is given by:

$$J_j = \begin{bmatrix} \alpha_i^1 & \alpha_i^2 & \alpha_i^3 \\ \beta_i^1 & \beta_i^2 & \beta_i^3 \\ \gamma_i^1 & \gamma_i^2 & \gamma_i^3 \end{bmatrix}, \tag{13}$$

where

$$\begin{cases} \alpha_i^j = \alpha_0^j + \sum\limits_{i=0}^{n} \frac{\Gamma(n-i+q_1(i))}{\Gamma(n-i+1)\Gamma(q_1(i))}(-\alpha_i^j - 1.4\alpha_i^j(1-(tanh(x_1(i)))^2) + 1.2\beta_i^j(1-(tanh(x_2(i)))^2) \\ \quad -7\gamma_i^j(1-(tanh(x_3(i)))^2)), \\ \beta_i^j = \beta_0^j + \sum\limits_{i=0}^{n} \frac{\Gamma(n-i+q_2(i))}{\Gamma(n-i+1)\Gamma(q_2(i))}(-\beta_i^j + 1.1\alpha_i^j(1-(tanh(x_1(i)))^2) + 2.8\gamma_i^j(1-(tanh(x_3(i)))^2)), \\ \gamma_i^j = \gamma_0^j + \sum\limits_{i=0}^{n} \frac{\Gamma(n-i+q_3(i))}{\Gamma(n-i+1)\Gamma(q_3(i))}(-\gamma_i^j + P\alpha_i^j(1-(tanh(x_1(i)))^2) - 2\beta_i^j(1-(tanh(x_2(i)))^2) \\ \quad +4\gamma_i^j(1-(tanh(x_3(i)))^2)), \end{cases} \tag{14}$$

$j = 1, 2, 3.$

Finally, the maximum L.E has the following formula:

$$\lambda_k(x_0) = \lim_{i\to\infty} \frac{1}{i} ln \mid \lambda_k^{(i)} \mid, \qquad for\ k = 1, 2, 3. \tag{15}$$

Note that λ_k are the eigenvalues of the matrix J_j.

As can be observed in the bifurcation and the Maximum L.E represented in Figure 3 and Figure 4, respectively, upon varying the parameter P, system (10) exhibits complex dynamics which include chaos and quasi-periodic behavior. In particular, system (10) is chaotic when the parameter $P \in [0.56, 0.61]$, where the value of the maximum Lyapunov exponents is positive, while for the rest of values of the parameter P, the system is quasi-periodic since it can not be periodic because fractional order systems cannot have periodic non-constant solutions (for more details, see [44–46]), where the value of the maximum Lyapunov exponents is negative.

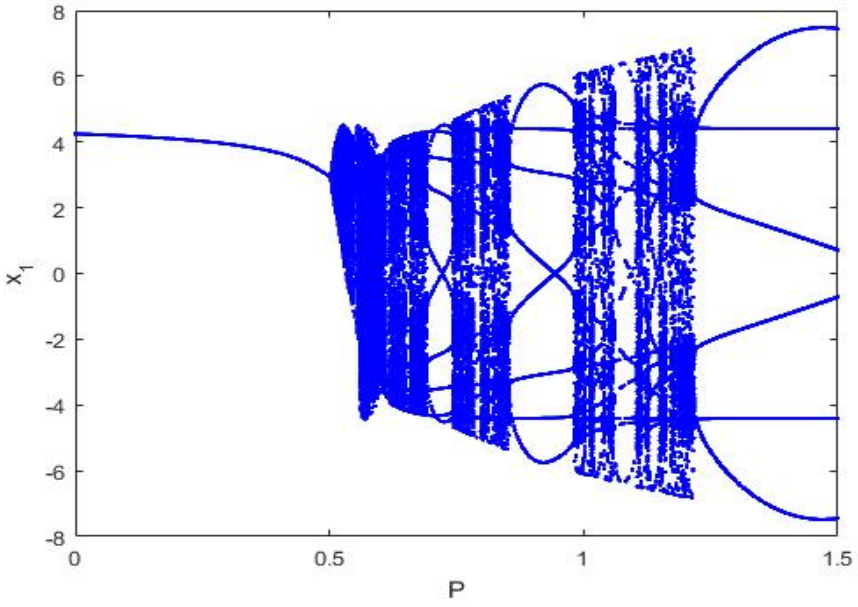

Figure 3. Bifurcation diagram versus the parameter P of the D.T.H.N.N with incommensurate fractional V.O (10).

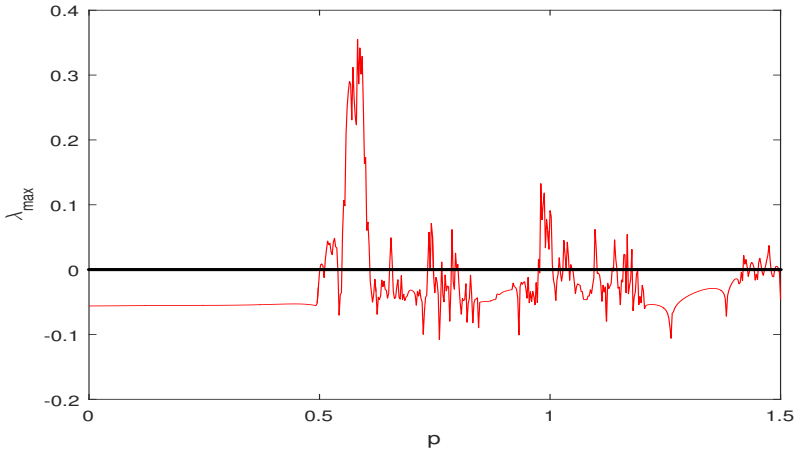

Figure 4. Maximum Lyapunov exponents versus P of D.T.H.N.N with incommensurate fractional V.O (10).

3.3. C_0 Complexity

To analyse the complex behaviour of systems, the C_0 complexity [47] is used based on the inverse Fourier transform.

For a sequence $[\phi(0), ..., \phi(M-1)]$, the algorithm of the C_0 complexity is given as follows:

- We calculate the discrete Fourier transform of the sequence $[\phi(0), ..., \phi(M-1)]$ as:

$$\Phi_M(m) = \sum_{j=0}^{M-1} \phi(j) \exp^{-2\pi i(jm/M)}, \qquad m = 0, ..., M-1. \tag{16}$$

- The mean square value is given as:

$$G_M = \frac{1}{M} \sum_{m=0}^{M-1} |\Phi_M(m)|^2. \tag{17}$$

- We set

$$\bar{\Phi}_M(m) = \begin{cases} \Phi_M(m) & if \quad |\Phi_M(m)|^2 > rG_M, \\ 0 & if \quad |\Phi_M(m)|^2 \leq rG_M. \end{cases} \tag{18}$$

- We define the inverse Fourier transform of $\bar{\Phi}_M$ as follows:

$$\bar{\phi}(j) = \frac{1}{M} \sum_{m=0}^{M-1} \bar{\Phi}(m) \exp^{2\pi i(jm/M)}, \qquad j = 0, ..., M-1. \tag{19}$$

Finally, the formula of the C_0 complexity is defined as:

$$C_0 = \frac{\sum_{j=0}^{M-1} |\phi(j) - \bar{\phi}(j)|^2}{\sum_{j=0}^{M-1} |\phi(j)|^2}. \tag{20}$$

The plot of C_0 complexity is shown in Figure 5, and we can observe that the value of the C_0 complexity of the proposed system (10) increases when the parameter P passes through the range [0.56, 0.61], which confirms that the proposed system is chaotic in this range, so the C_0 algorithm measures the complexity effectively.

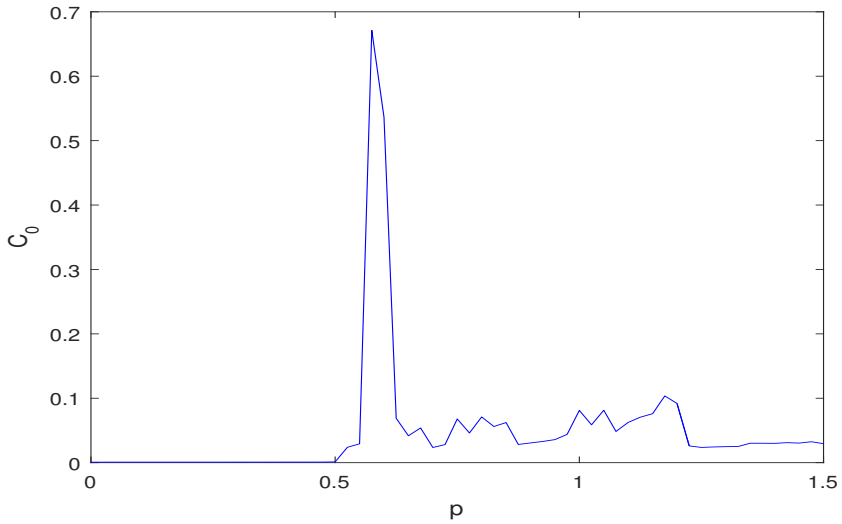

Figure 5. The C_0 complexity versus P of the D.T.H.N.N with incommensurate V.O (10).

3.4. The 0-1 Test Method for Chaos

Another method that can be used to test chaos of the proposed D.T.H.N.N with incommensurate fractional V.O is a "0–1 test", which was first presented by Gottwald and Melbourne [48] to detect the existence of chaos from a time series.

Firstly, we consider a time series $(w(i))_{i=1,...,N}$ and c a random constant in the interval $(0, \pi)$. Then, we define two translation variables as follows:

$$p_c(m) = \sum_{i=1}^{m} w(i)cos(ic), q_c(m) = \sum_{i=1}^{m} w(i)sin(ic), \qquad m = 1, 2, ..., N. \tag{21}$$

In addition, we present the formula of the mean square displacement:

$$M_c(m) = \frac{1}{N}\sum_{i=1}^{N}((p_c(i+m) - p_c(i))^2 + (q_c(i+m) - q_c(i))^2), \qquad m < \frac{N}{10}. \tag{22}$$

Finally, the asymptotic growth rate is defined by:

$$K_c = \lim_{m\to\infty} \frac{\log M_c}{\log m}. \tag{23}$$

Now, in order to determine the presence of chaos, we need the plot of the asymptotic growth rate $K = median(K_c)$ and the plot of q_c and p_c in the $p - q$ plane. When K is closer to 1 and the trajectories of q_c and p_c are Brownian, the map is chaotic, whereas, when K is closer to 0 and the trajectories of q_c and p_c are bounded, the map is regular.

Figure 6 depicts the 0–1 test versus P of the D.T.H.N.N with an incommensurate fractional variable order (10). One can observe that, when $P \in [0.56, 0.61]$, the value of the growth rate K is closer to 1, which indicates the presence of chaos, while the value of the growth rate K is closer to 0 for the rest of values of the system parameter P, which proves that the proposed system (10) is quasi-periodic.

The $p_c - q_c$ plots are shown in Figure 7 for different values of the parameter P with the same initial conditions used previously. In particular, when $P = 0.1$ and $P = 0.7$, the trajectories of q_c and p_c are bounded, and the system (10) is quasi-periodic. When $P = 0.59$ and $P = 0.6$ the trajectories of q_c and p_c are Brownian and the system (10) is chaotic, which is extremely similar to the results obtained in Figure 6.

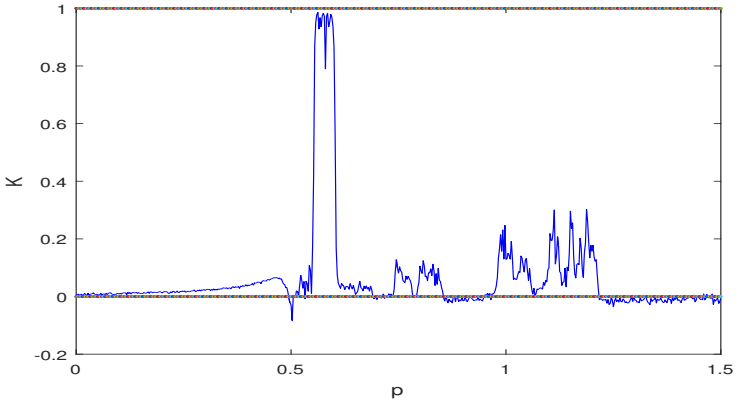

Figure 6. The 0-1 test versus P of the D.T.H.N.N with incommensurate fractional V.O (10).

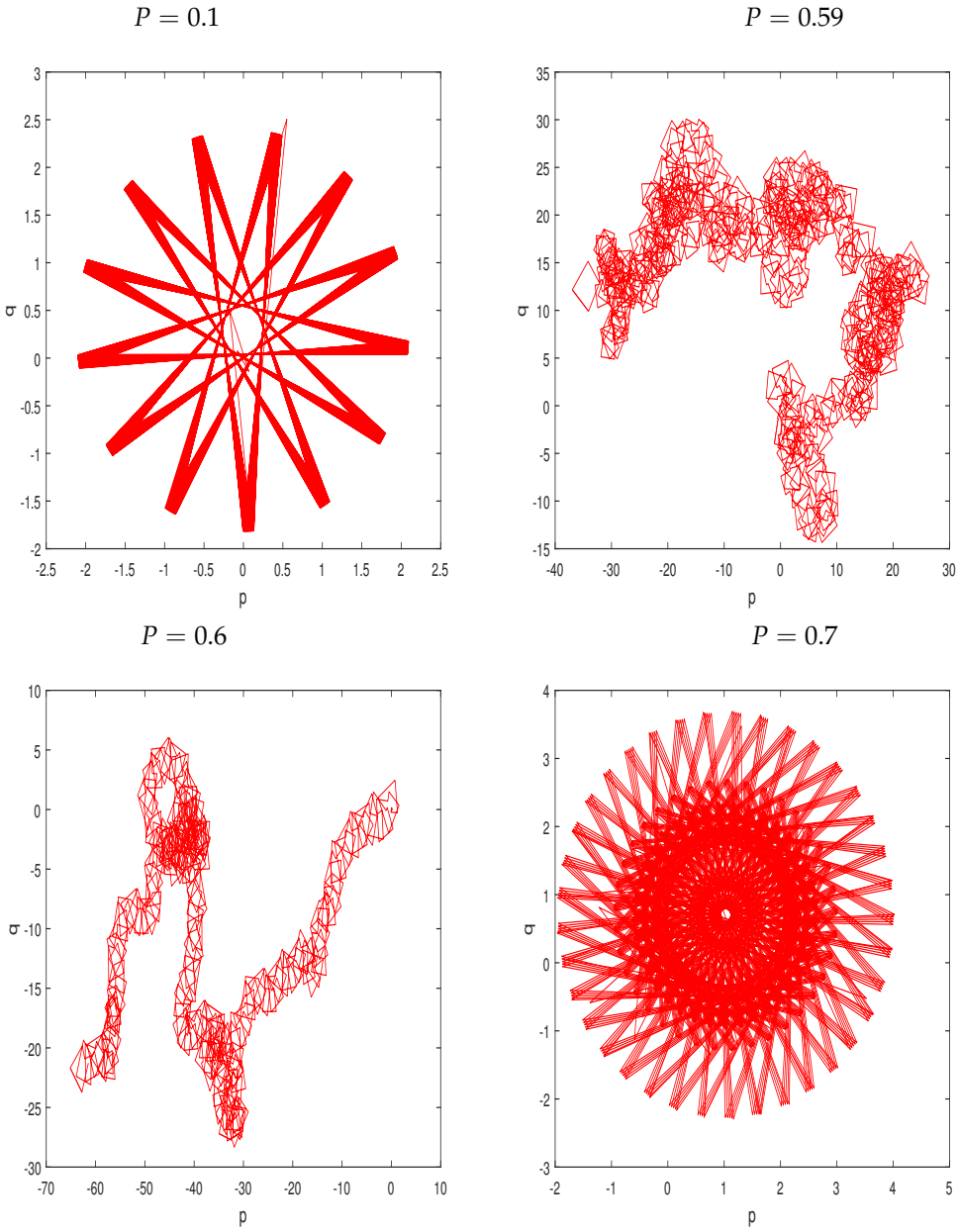

Figure 7. The plot of p versus q for the D.T.H.N.N with incommensurate fractional V.O (10) for different values of the system parameter P.

We observe that the results of the 0-1 test agree well with the results obtained in bifurcation and the largest Lyapunov exponents' diagrams and the C_0 complexity algorithm.

4. Conclusions and Future Research Directions

Based on the discrete time Hopfield neural network with incommensurate fractional order, this research has presented a Caputo-difference form of the discrete time Hopfield neural network with an incommensurate fractional variable-order. Phase-plot portraits, bifurcation and maximum Lyapunov exponents diagrams have shown the complexity of the dynamics of the proposed model. In addition, the 0-1 test and C_0 complexity algorithm have been employed to prove and confirm the presence of chaos in a small interval. The obtained results give us insight into the behavior of the discrete time Hopfield neural network system when using fractional variable order.

The future research directions that will depend on the results obtained in this work are in two directions: the first is theoretical and the second is practical. The theoretical aspect lies in the formulation of discrete time neural networks with strong and appropriate fractional operators, whether from an analytical or numerical point of view, while the practical aspect lies in the actual application of this type of network, especially in encryption and secure communications; the authors also aim to find electrical circuits that represent this type of network, due to the dynamic property of these neural networks proven to be suitable for these types of applications.

Author Contributions: Formal analysis, R.C.K., A.O., M.A.H. and G.G.; Investigation, A.O. and M.A.H.; Methodology, A.O. and G.G.; Software, R.C.K.; Supervision, A.O. and M.A.H.; Validation, A.O. and G.G.; Writing—original draft, R.C.K. All authors have read and agreed to the published version of the manuscript.

Funding: This research received no external funding.

Informed Consent Statement: Informed consent was obtained from all subjects involved in the study.

Data Availability Statement: The data presented in this study are available on request from the references.

Conflicts of Interest: The authors declare no conflict of interest.

References

1. Kocarev, L.; Szczepanski, J.; Amigo, J.M.; Tomovski, I. Discrete Chaos—I: Theory. *IEEE Trans. Circuits Syst. I Regul. Pap.* **2006**, *53*, 1300–1309. [CrossRef]
2. Li, C.; Song, Y.; Wang, F.; Liang, Z.; Zhu, B. Chaotic path planner of autonomous mobile robots based on the standard map for surveillance missions. *Math. Prob. Eng.* **2015**, *2015*, 263964. [CrossRef]
3. Papadimitriou, S.; Bezerianosa, A.; Bountis, T.; Pavlides, G. Secure communication protocols with discrete nonlinear chaotic maps. *J. Syst. Archit.* **2001**, *47*, 61–72. [CrossRef]
4. Kwok, H.S.; Tang, W.K.S.; Man, K.F. Online secure chatting system using discrete chaotic map. *Int. J. Bifurcat. Chaos* **2004**, *14*, 285–292. [CrossRef]
5. Banerjee, S.; Kurth, J. Chaos and cryptography: A new dimension in secure communications. *Eur. Phys. J. Spec. Top.* **2014**, *223*, 1441–1445. [CrossRef]
6. Fataf, N.A.A.; Mukherjee, S.; Said M.R.M.; Rauf, U.F.A.; Hina A.D.; Banerjee S. Synchronization between two discrete chaotic systems for secure communications. *Int. Conf. Comms. Elec. (ICCE)* **2016**, 477–481. [CrossRef]
7. Hénon M. A two-dimensional mapping with a strange attractor. *Commun. Math. Phys.* **1976**, *50*, 69–77. [CrossRef]
8. Lozi, R. Un atracteur étrange du type attracteur de Hénon. *J. Phys. Colloq.* **1978**, *39*, 9–10.:1978505. [CrossRef]
9. Zeraoulia, E.; Sprott J.C. The discrete hyperchaotic double scroll, *Int. J. Bifurc. Chaos.* **2009**, *19*, 1023–1027. [CrossRef]
10. Hitzl, D.L.; Zele, F. An exploration of the Hénon quadratic map. *Phys. D Nonlinear Phenom.* **1985**, *14*, 305–326. [CrossRef]
11. Baier, G.; Sahle, S. Design of hyperchaotic flows. *Phys. Rev. E* **1995**, *51*, 2712–2714. [CrossRef] [PubMed]
12. Yan, Z. (complete or anticipated) synchronization backstepping scheme in a class of discrete–time chaotic (hyperchaotic) systems : A symbolic–numeric computation approach. *Chaos* **2006**, *16*, 1930727. [CrossRef] [PubMed]
13. Ouannas, A.; Bendoukha, S.; Khennaoui, A.A.; Grassi, G.; Wang, X.; Pham, V.T. Chaos synchronization of fractional-order discrete-time systems with different dimensions using two scaling matrices. *Open Phys. J.* **2019**, *17*, 942–949. [CrossRef]
14. Podlubny, I. *Fractional Differential Equations: An Introduction to Fractional Derivatives, Fractional Differential Equations, to Methods of Their Solution and Some of Their Applications*; Elsevier: Amsterdam, The Netherlands, 1999; ISBN 9780080531984. [CrossRef]

15. Ostalczyk, P. *Discrete Fractional Calculus: Applications in Control and Image Processing*; World Scientific: Singapore, 2015. [CrossRef]
16. Atici, F.M.; Eloe, P. Discrete fractional calculus with the nabla operator. *Electron. J. Qual. Theory Differ. Equ.* **2009**, *2009*, 1–12. [CrossRef]
17. Diaz, J.B.; Osler, T.J. Differences of fractional order. *Math. Comput.* **1974**, *28*, 185–202. [CrossRef]
18. Wu, G.C.; Baleanu, D. Discrete fractional logistic map and its chaos. *Nonlinear Dyn.* **2014**, *75*, 283–287. [CrossRef]
19. Khennaoui, A.A.; Ouannas, A.; Bendoukha, S.; Grassi, G.; Wang, X.; Pham, V.T.; Alsaadi, F.E. Chaos, control, and synchronization in some fractional-order difference equations. *Adv. Differ. Equ.* **2019**, *2019*, 412. [CrossRef]
20. Khennaoui, A.A.; Ouannas, A.; Bendoukha, S.; Grassi, G.; Lozi, R.P.; Pham, V.T. On Fractional Order Discrete Time Systems: Chaos, Stabilization and Synchronization. *Chaos Solit. Fractals* **2019**, *119*, 150–162. [CrossRef]
21. Ouannas, A.; Khennaoui, A.A.; Odibat, Z.; Pham, V.T.; Grassi, G. On the dynamics, control and synchronization of fractional-order Ikeda map. *Chaos Solit. Fractals* **2019**, *123*, 108–115. [CrossRef]
22. Ouannas, A.; Khennaoui, A.A.; Momani, S.; Grassi, G.; Pham, V. T.; El-Khazali, R.; Vo Hoang, D. A Quadratic Fractional Map without Equilibria: Bifurcation, 0-1 Test, Complexity, Entropy, and Control. *Int. J. Electron.* **2020**, *9*, 748. [CrossRef]
23. Ouannas, A.; Almatroud, O.A.; Khennaoui, A.A.; Al-sawalha, M.M.; Baleanu, D.; Huynh, V.V.; Pham, V.T. Bifurcations, Hidden Chaos and Control in Fractional Maps. *Symmetry* **2020**, *12*, 879. [CrossRef]
24. Hadjabi, F.; Ouannas, A.; Shawagfeh, N.; Khennaoui, A.A.; Grassi, G. On Two-Dimensional Fractional Chaotic Maps with Symmetries. *Symmetry* **2020**, *12*, 756. [CrossRef]
25. Abdeljawad, T. On Riemann and Caputo fractional differences, *Comput. Math. Appl.* **2011**, *62*, 1602–1611. [CrossRef]
26. Wang, H.; Yu, Y.; Wen, G. Stability analysis of fractional-order Hopfield neural networks with time delays. *Neural Netw.* **2014**, *55*, 98–109. [CrossRef] [PubMed]
27. Lazarević, M. Stability and stabilization of fractional order time delay systems. *Sci. Tech. Rev.* **2011**, *61*, 31–45.
28. Chen, L.; Chai, Y.; Wu, R.; Ma, T.; Zhai, H. Dynamic analysis of a class of fractional-order neural networks with delay. *Neurocomputing* **2013**, *111*, 190–194. [CrossRef]
29. Liu, H.; Li, S.; Wang, H.; Huo, Y.; Luo, J. Adaptive synchronization for a class of uncertain fractional-order neural networks. *Entropy* **2015**, *17*, 7185–7200. [CrossRef]
30. Xi, Y.; Yu, Y.; Zhang, S.; Hai, X. Finite-time robust control of uncertain fractional-order Hopfield neural networks via sliding mode control. *Chin. Phys. B* **2018**, *27*, 010202. [CrossRef]
31. Zhang, S.; Yu, Y.; Yu, J. LMI conditions for global stability of fractional-order neural networks. *IEEE Trans. Neural Netw. Learn. Syst.* **2016**, *28*, 2423–2433. [CrossRef]
32. Roohi, M.; Zhang, C.; Chen, Y. Adaptive model-free synchronization of different fractional-order neural networks with an application in cryptography. *Nonlinear Dyn.* **2020**, *100*, 3979–4001. [CrossRef]
33. Chen, L.; Chai, Y.; Wu, R.; Yang, J. Stability and stabilization of a class of nonlinear fractional-order systems with Caputo derivative. *IEEE Trans. Circuits Syst. II* **2012**, *59*, 602–606. [CrossRef]
34. Ahn, H.S.; Chen, Y. Necessary and sufficient stability condition of fractional-order interval linear systems. *Automatica* **2008**, *44*, 2985–2988. [CrossRef]
35. Farges, C.; Moze, M.; Sabatier, J. Pseudo state feedback stabilization of commensurate fractional order systems. In Proceedings of the 2009 European Control Conference (ECC), Budapest, Hungary, 23–26 August 2009; pp. 3395–3400. [CrossRef]
36. Utkin, V.I. Sliding mode control in discrete-time and difference systems. *Var. Struct. Lyapunov Control* **1994**, *193*, 87–107. [CrossRef]
37. Slotine, J.J.; Li, W. Adaptive strategies in constrained manipulation. In Proceedings of the 1987 IEEE International Conference on Robotics and Automation, Raleigh, NC, USA, 31 March–3 April 1987; pp. 595–601. [CrossRef]
38. Ouannas, A.; Khenaoui, A.A.; Almatroud, A.O.; Gasri, A.; Al-Sawalha, M.M.; Jahanshahi, H. Coexisting Behaviors of Asymmetric Attractors in New Fractional Discrete-Time Neural Network with Variable Order and Short Memory Effect: Chaos, Complexity and Multistability. *in press*.
39. Kaslik, E.; Racdulescu, I.R. Dynamics of complex-valued fractional-order neural networks. *Neural Netw.* **2017**, *89*, 39–49. [CrossRef]
40. Abbes, A.; Ouannas, A.; Shawagfeh, N.; Khennaoui, A.A. Incommensurate Fractional Discrete Neural Network: Chaos and complexity. *Eur. Phys. J. Plus* **2022**, *137*, 235. [CrossRef]
41. Kaslik, E.; Sivasundaram, S. Nonlinear dynamics and chaos in fractional-order neural networks. *Neural Netw.* **2012**, *32*, 245–256. [CrossRef]
42. Chen, F.; Luo, X.; Zhou, Y. Existence results for nonlinear fractional difference equation. *Adv. Differ. Equation* **2011**, *2011*, 713201 [CrossRef]
43. Wu, G.C.; Baleanu, D. Jacobian matrix algorithm for Lyapunov exponents of the discrete fractional maps. *Commun. Nonlinear Sci. Numer. Simul.* **2015**, *22*, 95–100. [CrossRef]
44. Tavazoei, M.S.; Haeri, M. A proof for non existence of periodic solutions in time invariant fractional order systems. *Automatica* **2009**, *45*, 1886–1890. [CrossRef]
45. Tavazoei, M.S. A note on fractional-order derivatives of periodic functions. *Automatica* **2010**, *46*, 945–948. [CrossRef]
46. Zhang, X. Relationship Between Integer Order Systems and Fractional Order Systems and Its Two Applications. *IEEE/CAA J. Autom. Sin.* **2018**, *5*, 639–643. [CrossRef]

47. Ran, J. Discrete chaos in a novel two-dimensional fractional chaotic map. *Adv. Differ. Equation* **2018**, *2018* , 294. [CrossRef]
48. Gottwald, G.A.; Melbourne, I. A new test for chaos in deterministic systems. *Proc. Math. Phys. Eng. Sci.* **2004**, *460* , 603–611. [CrossRef]